Available online at www.sciencedirect.com
SCIENCE DIRECT®
Physica E 22 (2004) 538–541
PHYSICA E
www.elsevier.com/locate/physe

Electron spin redistribution in a Kondo quantum dot in the low-magnetic-field regime

W.G. van der Wiel[a,b,*], M. Stopa[c], S. De Franceschi[d], L.P. Kouwenhoven[d], S. Tarucha[e]

[a] *PRESTO-JST; University of Tokyo, 7-3-1, Hongo, Bunkyo-ku, Tokyo 113-0033, Japan*
[b] *Department of NanoScience and DIMES, Delft University of Technology, PO Box 5046, GA Delft 2600, The Netherlands*
[c] *ERATO-JST, 3-1 Morinosato-Wakamiya, Atsugi-shi Kanagawa-ken 243-0198, Japan*
[d] *ERATO-JST, Department of NanoScience and DIMES, Delft University of Technology, PO Box 5046, GA Delft 2600, The Netherlands*
[e] *ERATO-JST, University of Tokyo, 7-3-1, Hongo, Bunkyo-ku, Tokyo 113-0033, Japan*

Abstract

We observe an alternation of high and low valley conductance regions as a function of magnetic field for constant electron number in a Kondo quantum dot. The valley conductance also alternates between high and low as a function of electron number at constant magnetic field. Full 3D spin density functional calculations of our device quantitatively explain this behaviour in terms of a spatial redistribution of the electron spins in the dot. The spin density functional calculations provide a connection between the many-body state of the Kondo effect on the one hand, and the detailed electronic structure of our nanoscale device on the other hand.

PACS: 73.23.−b; 73.23.Hk; 72.15.Qm

Keywords: Electron spin; Kondo effect; Quantum dots; Spin density functional calculations

1. Introduction

The Kondo effect [1] was originally observed in metals that contain a small concentration of magnetic impurities. The phenomenon occurs because below a certain temperature, which is called the Kondo temperature, T_K, the mobile electrons in the host metal tend to screen the non-zero total spin of the electrons in the magnetic impurity atom. A finite net total electron spin confined in a quantum dot [2] connected to source and drain leads, can nicely mimic the situation of a localized spin impurity surrounded by a Fermi sea. This analogy led to the prediction that the Kondo effect should occur in quantum dot systems as well [3,4].

The Kondo effect in quantum dots gives rise to an enhanced conductivity in the Coulomb blockade regime (as opposed to an enhanced *resistivity* in the case of a metal containing magnetic impurities) and occurs for temperatures and source–drain voltages below an energy scale set by T_K. The first

* Corresponding author. University of Tokyo, PRESTO-JST, 7-3-1 Hongo, Bunkyo-ku, Tokyo 113-0033, Japan. Fax: +81-3-5841-4162.
E-mail address: wilfred@tomoko.phys.s.u-tokyo.ac.jp (W.G. van der Wiel).

1386-9477/$ - see front matter © 2003 Elsevier B.V. All rights reserved.
doi:10.1016/j.physe.2003.12.064

experimental results on the Kondo effect in quantum dots [5–7] were described with help of the spin-$\frac{1}{2}$ Anderson impurity model. If spin-degenerate single-particle levels are consecutively filled, the dot has either total electron spin $S = 0$ (for electron number N even) or $S = \frac{1}{2}$ (for N odd). In that case, the Kondo effect is only expected for odd N, giving rise to an "odd–even-effect" in the Coulomb valley conductance. However, many experiments have shown results that deviate from the scenario sketched above [8–18].

Here, we are particularly interested in the so-called "chessboard pattern" in the dot conductance as a function of magnetic field, B, and gate voltage, V_g [12,13,15–18]. This pattern is characterized by the alternation of high and low valley conductance regions as a function of B within the same Coulomb valley, i.e. for *constant* N. The conductance also alternates when N is changed by sweeping V_g at constant B. When the conductance is plotted in greyscale (see Fig. 1c), some similarity with the fields of a chessboard can be found, giving rise to the name of this phenomenon. Experiments have shown that the enhanced conductance in certain Coulomb blockade regions can be ascribed to the Kondo effect, for both N odd and even [12,13,15–18].

In this paper, we present full 3D spin density functional (SDF) calculations for our quantum dot structure. The analysis of the total electron angular momentum and the spatial spin distribution gives a good insight in the behaviour of our device in the low-magnetic-field regime. In addition, we introduce an effective Kondo coupling, derived entirely from the self-consistent results. Hence we can simultaneously calculate the electronic states of the dot and an estimate of the Kondo coupling exhibiting the chessboard structure. Our calculations clearly show that the underlying mechanism of the chessboard pattern is formed by the redistribution of electron spins between the two lowest (spin-degenerate) Landau levels (LLs) in the dot. An interesting finding is that higher LLs only start to fill below a few tenths of a Tesla, due to the small electron number and shallow potential in the dot. Recent experimental and theoretical work [19] has also focused on electron spin redistribution in quantum dots particularly in the filling-factor-two-regime, however, without addressing the Kondo effect.

2. Experiment

Our quantum dot device is shown in Fig. 1a [20]. By depleting the 2D electron gas below the metal gates, a single quantum dot is defined. The electron number is varied by sweeping the right gate voltage, V_{g3}. The self-consistently calculated potential landscape in the relevant area is shown in Fig. 1b. The SDF calculations show that our dot typically contains $\sim$ 20–40 electrons.

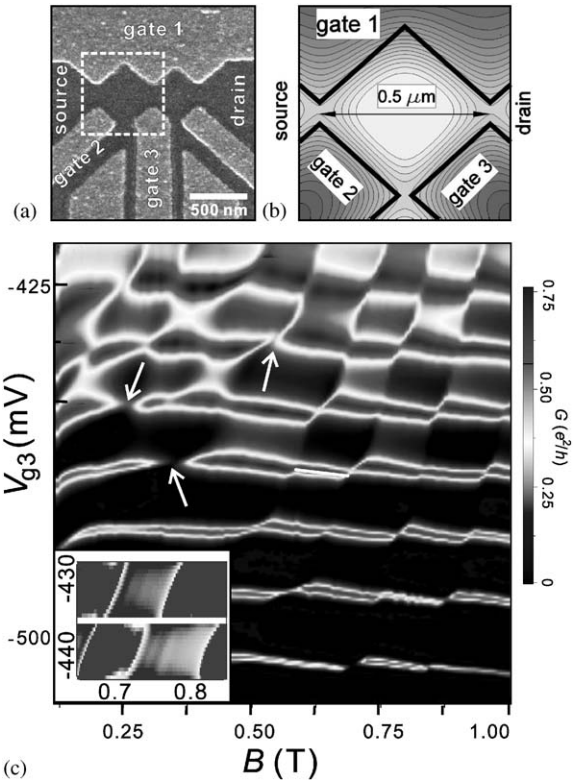

Fig. 1. (a) Scanning electron micrograph of the device, used to create a single quantum dot. The relevant region is indicated by a dashed box and the used gate electrodes (light grey) are indicated. Ungated 2DEG mobility is 2.3×10^6 cm^2/(V s) and electron density is 1.9×10^{15} m^{-2} at 4.2 K. Nominal dot size is 320×320 nm^2. (b) Calculated self-consistent potential landscape of the single dot. Lowest contour corresponds to -6 meV, spacing of contours is 9 meV. (c) Greyscale plot of the experimental linear conductance G through dot as function of B and V_{g3} at 10 mK. White arrows indicate some regions where Coulomb peak suppression occurs. Inset, calculated chessboard pattern using the Kondo parameter K (see text).

Fig. 1c shows a greyscale plot of the linear conductance G through the dot as a function of B and V_{g3}. For the most negative values of V_{g3} the dot-lead coupling is weak. As a result relatively sharp Coulomb peaks and low valley conductance are observed. For more positive V_{g3} values, the valley conductance reaches $\sim e^2/h$ in certain regions of the (B, V_{g3}) plane. The regions of low and high valley conductance alternate both along the V_{g3} and the B-axis in a regular way, resulting in a chessboard pattern as mentioned above. The V_{g3} period ($\sim$ 10 mV) is set by the energy required for adding an extra electron to the dot (addition energy), whereas the B period ($\sim$ 0.1 T) corresponds to adding a flux quantum to the effective dot area. Based on the temperature dependence of G in the high valley conductance regions (not shown), the enhanced G is ascribed to the Kondo effect. The transition from high to low valley conductance is associated with a sudden jump of the V_{g3} position of the Coulomb peaks. In some cases (see white arrows in Fig. 1c) the jump is accompanied by a suppression of the peak height [18]. We present below a quantitative explanation for some of the main features of our experimental results based on full 3D spin density functional calculations.

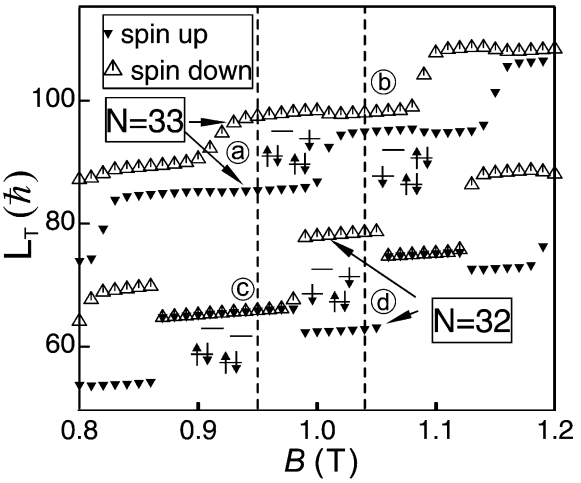

Fig. 2. Calculated total electron orbital angular momentum, L_T, as a function of B for both spin-up ($L_{T\uparrow}$) and spin-down ($L_{T\downarrow}$) in the cases of 32 ($V_{g1} = -410$ mV, $V_{g2} = -392$ mV, $V_{g3} = -449$ mV) and 33 (V_{g3} changed to -440 mV) electrons. Spin-down is assumed to have lower Zeeman energy. The two dashed lines mark B=0.95 and 1.04 T. The positions along the dashed lines indicated by a–d correspond to the net spin distributions given in Fig. 3a–d, respectively, and are explained in the text. Schematic occupancy configurations (energy vs. position) of the uppermost levels in both LLs (LL1: right; LL2: left) at the dot boundary are given at positions a–d.

3. Spin density functional calculations

We self-consistently compute eigenvalues $\varepsilon_{p\sigma}$, eigenfunctions $\psi_{p\sigma}$, occupancies $n_{p\sigma}$, and tunneling coefficients $\gamma_{p\sigma}$, with p the orbital and σ the spin indices, as well as the total interacting energy F of the dot–gate–leads system, all as a function of N, V_{g3} and B [18,21]. Fig. 2 shows a graph of the expectation value of the total electron orbital angular momentum, L_T, for both spin species versus B for N=32,33. Only the first two LLs in the dot are occupied. The lowest LL (LL1) is most strongly coupled to the leads, whereas the higher LL (LL2) is more confined in the dot centre and hence much less effectively coupled to the leads [13,18,22]. Therefore, instead of the total net spin in the dot, it is much more the net spin in the lowest (i.e. outer LL) that matters for the Kondo physics [18].

When B increases, spin-down and spin-up electrons successively move from the inner to the outer LL, thereby increasing their angular momentum. At (a) (see Fig. 2) the number of electrons in the inner LL, N_2, is even, and necessarily the number of electrons in the outer LL, N_1, is odd. As spin-down is assumed to have the lowest Zeeman energy, the unpaired electron in LL1 has spin-down, leading to the larger L_T for spin-down ($L_{T\downarrow}$) at (a). The difference $L_{T\downarrow} - L_{T\uparrow}$ is relatively large, because the unpaired electron is occupying the LL with the highest orbital angular momentum. At (b) there is an unpaired spin-down electron in LL2, leading to a smaller value of $L_{T\downarrow} - L_{T\uparrow}$. For N=32 at (c), there is no excess spin in either of the LLs, resulting in $L_{T\downarrow} \approx L_{T\uparrow}$. When B is increased to position (d) not only $L_{T\downarrow}$ increases, but also $L_{T\uparrow}$ *decreases*. The reason is that the transition of a spin-down electron from LL2 to LL1 is accompanied by a spin flip of the unpaired spin-up electron in LL2, favoured by the lower Zeeman energy and, to a lesser extent, by the gain in exchange energy. The expectation value of the net spin per area, $S(x, y)$, defined as

$$S(x,y) = \sum_{p=1}^{\infty} (n_{p\downarrow}|\psi_{p\downarrow}|^2 - n_{p\uparrow}|\psi_{p\uparrow}|^2), \qquad (1)$$

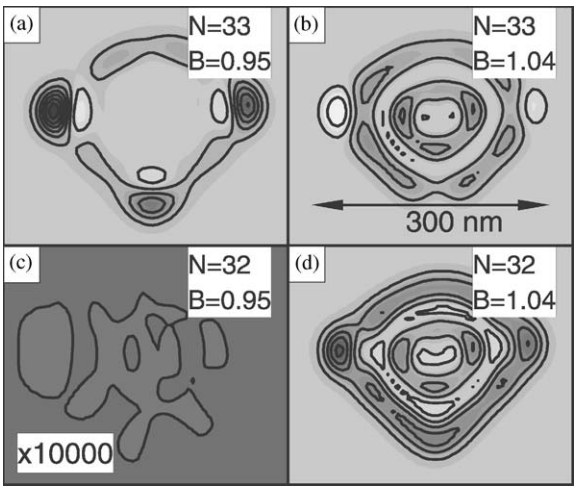

Fig. 3. Calculated greyscale-contour plot of the net spin per area, $S(x, y)$. The scale ranges from -6 (light grey) to 21 milliparticles per 100 nm^2 (black). Magnetic field values are in tesla. Plots a–d correspond to the positions indicated in Fig. 2. Note that the plots are not symmetric due to the asymmetric dot shape and asymmetrically applied gate voltages (see caption Fig. 2).

corresponding to situations (a)–(d) of Fig. 2, is given in Fig. 3. Fig. 3a clearly shows that the net spin (down) density is concentrated along the periphery of the dot, especially in the regions closest to the leads. In Fig. 3b, however, the net spin density close to the leads is significantly lower than in the region closer to the centre. Although $N = 33$ (i.e. odd) in both cases, the electron spin redistribution effectively suppresses the Kondo effect in the second case, as we will quantify below in some more detail. In situation (c) we do not expect any finite net spin anywhere in the dot, which is reflected in Fig. 3c (note that $S(x, y)$ is magnified 10^4 times). On the other hand, in Fig. 3d, there is again a strong concentration of spin at the edges of the dot, turning on the Kondo effect.

In order to quantitatively show that the spin redistribution indeed gives rise to the experimentally observed chessboard pattern, we introduce as a measure of the Kondo conductance the sum K of all co-tunneling amplitudes that leave the ground state unchanged except for the flip of a single spin $K \equiv \sum_{p,\sigma} n_{p,\sigma}(1 - n_{p,\bar{\sigma}})\sqrt{\gamma_{p,\sigma}\gamma_{p,\bar{\sigma}}}(1/E_C^N - 1/E_C^{N-1})$ where $E_C^N \equiv F(N + 1, V_{g3}, B) - F(N, V_{g3}, B)$ and $\bar{\sigma}$ is the spin opposite to σ [18]. K calculated for a small (B, V_{g3}) region is shown in the inset to Fig. 1c, indeed revealing the expected valley conductance alternation.

4. Summary

Using full 3D spin density functional calculations we have been able to *quantitatively* explain the underlying mechanism of the chessboard pattern in the conductance of a Kondo quantum dot—as experimentally observed by us and many other groups—in terms of magnetically induced spin redistribution.

Acknowledgements

We acknowledge financial support from the DARPA grant number DAAD19-01-1-0659 of the QuIST program.

References

[1] J. Kondo, Prog. Theor. Phys. 32 (1964) 37.
[2] L.P. Kouwenhoven, et al., Electron transport in quantum dots, in: L.L. Sohn, et al. (Eds.), Mesoscopic Electron Transport Series E, Vol. 345, Kluwer, Dordrecht, 1997, pp. 105–214.
[3] L.I. Glazman, M.E. Raikh, JETP Lett. 47 (1988) 452.
[4] T.K. Ng, P.A. Lee, Phys. Rev. Lett. 61 (1988) 1768.
[5] D. Goldhaber-Gordon, et al., Nature 391 (1998) 156.
[6] S.M. Cronenwett, et al., Science 281 (1998) 540.
[7] J. Schmid, et al., Physica B 256–258 (1998) 182.
[8] S.M. Maurer, et al., Phys. Rev. Lett. 83 (1999) 1403.
[9] W.G. van der Wiel, et al., Science 289 (2000) 2105.
[10] S. Sasaki, et al., Nature 405 (2000) 764.
[11] J. Nygård, et al., Nature 408 (2000) 342.
[12] J. Schmid, et al., Phys. Rev. Lett. 84 (2000) 5824.
[13] M. Keller, et al., Phys. Rev. B 64 (2001) 033302.
[14] W.G. van der Wiel, et al., Phys. Rev. Lett. 88 (2002) 126803.
[15] D. Sprinzak, et al., Phys. Rev. Lett. 88 (2002) 176805.
[16] C. Fühner, et al., Phys. Rev. B 66 (2002) 161305(R).
[17] U.F. Keyser, et al., Phys. Rev. Lett. 90 (2003) 196601.
[18] M. Stopa, et al., Phys. Rev. Lett. 91 (2003) 046601.
[19] M. Ciorga, et al., Phys. Rev. Lett. 88 (2002) 256804; A. Wensauer, et al., Phys. Rev. B 67 (2003) 035325.
[20] W.G. van der Wiel, et al., Rev. Mod. Phys. 75 (2003) 1.
[21] M. Stopa, Phys. Rev. B 54 (1996) 13767; M. Stopa, Semicond. Sci. Technol. 13 (1998) A55; M. Stopa, Physica E 10 (2001) 103.
[22] P.L. McEuen, et al., Phys. Rev. B 45 (1992) 11419; J.M. Kinaret, N.S. Wingreen, Phys. Rev. B 48 (1993) 11113; A.K. Evans, L.I. Glazman, B.I. Shklovskii, Phys. Rev. B 48 (1993) 11120; N.C. van der Vaart, et al., Phys. Rev. Lett. 73 (1994) 320.